Dynamics of diluted Ho spin ice $Ho_{2-x}Y_xTi_2O_7$ studied by neutron spin echo spectroscopy and ac susceptibility

G. Ehlers
SNS Project, Oak Ridge National Laboratory, Building 8600, Oak Ridge, Tennessee 37831-6475, USA

J. S. Gardner
Physics Department, Brookhaven National Laboratory, Upton, New York 11973-5000, USA
and NIST Center for Neutron Research, NIST, Gaithersburg, Maryland 20899-8562, USA

C. H. Booth and M. Daniel
Chemical Sciences Division, Lawrence Berkeley National Laboratory, Berkeley, California 94720, USA

K. C. Kam and A. K. Cheetham
Materials Research Laboratory, University of California, Santa Barbara, California 93106, USA

D. Antonio, H. E. Brooks, and A. L. Cornelius
Physics Department, University of Nevada Las Vegas, Las Vegas, Nevada 89154-4002, USA

S. T. Bramwell and J. Lago
Department of Chemistry, University College London, 20 Gordon Street, London WC1H 0AJ, United Kingdom

W. Häussler
FRM II, Lichtenbergstrasse 1, 85747 Garching, Germany

N. Rosov
NIST Center for Neutron Research, NIST, Gaithersburg, Maryland 20899-8562, USA
(Received 6 March 2006; published 23 May 2006)

We have studied the spin relaxation in diluted spin ice $Ho_{2-x}Y_xTi_2O_7$ by means of neutron spin echo spectroscopy and ac susceptibility measurements. Remarkably, the geometrical frustration is *not* relieved by doping with nonmagnetic Y, and the dynamics of the freezing is unaltered in the spin echo time window up to $x \simeq 1.6$. At higher doping with nonmagnetic Y ($x \geq 1.6$) a new relaxation process at relatively high temperature (up to at least $T \simeq 55$ K) appears which is more than 10 times faster than the thermally activated main relaxation process. We find evidence that over the whole range of composition all Ho spins participate in the dynamics. These results are compared to ac susceptibility measurements of the diluted Ho and Dy spin ice systems, which show that at low temperature the Arrhenius behavior is masked by another dynamical process with little temperature dependence. X-ray absorption fine structure (EXAFS) spectra and x-ray diffraction show that the samples are structurally well ordered.

DOI: 10.1103/PhysRevB.73.174429 PACS number(s): 75.40.Gb, 75.25.+z, 75.50.Dd

Frustration is a general concept in physics to describe the effects that occur when competing interactions prevent a system from settling into a unique ground state. In magnetism, where temperature, magnetic field, and pressure are the relevant thermodynamic parameters, frustrated systems like spin glasses have been studied for many years. In geometrically frustrated magnets, which are structurally well ordered, but where the spatial arrangement of the magnetic moments (spins) on the lattice is incompatible with their interactions (exchange, dipole, anisotropy), new and unique low temperature spin states have been found.[1,2] These ground states include the three-dimensional, low temperature cooperative paramagnet, $Tb_2Ti_2O_7$,[3] coexistence of long range ordered and paramagnetic spins down to lowest temperature in $Gd_2Ti_2O_7$,[4,5] and the superconductor $Cd_2Re_2O_7$.[6] The rare earth pyrochlore compounds $Dy_2Ti_2O_7$ (DTO) and $Ho_2Ti_2O_7$ (HTO), commonly known as spin ice,[7–15] have interested physicists over the past decade.

In the pyrochlore structure (see Fig. 1) the rare earth magnetic moments reside on a sublattice of corner-sharing tetrahedra (on the 16*d* site which has trigonal site symmetry). Frustration is created by the single ion anisotropy which has its origin in the crystalline electric field (CEF). In this situation, both Dy^{3+} ($J=15/2$) and Ho^{3+} ($J=8$) ions are subject to a strong local Ising anisotropy, which aligns the moment parallel to a local trigonal axis. Correspondingly, the single ion ground states are in both cases doublets, with the two states almost identical to the $|M_J=\pm J\rangle$ states. For HTO, the anisotropy gap to the first excited state is $\simeq 220$ K.[16–18] The ferromagnetic exchange and dipole interactions are much smaller, on the order of $\simeq 2$ K,[10,11] hence completely dominated by the anisotropy and frustrated. Globally, the interac-

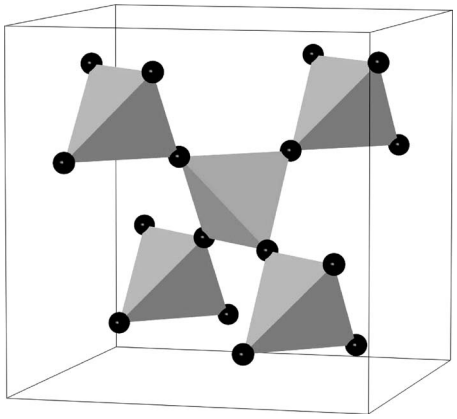

FIG. 1. The rare-earth sublattice of corner-sharing tetrahedra in the pyrochlore structure.

tion energies are minimized when two spins per tetrahedron are oriented to point inward and two point outward (ice rule). This is precisely analogous to the proton disorder in water ice.[19–21] A macroscopic ground state degeneracy results, as any state which obeys the ice rule for all tetrahedra is a ground state, and the spins freeze below $T \simeq 1$ K in a noncollinear disordered pattern showing only short-ranged ferromagnetic correlations.[12]

The dynamics of pure spin ice at temperatures $T > 1$ K has been studied using ac susceptibility and neutron spin echo techniques, and two important results have emerged.[9,22–25] First, at a given temperature only one global spin relaxation time is found in the system. Second, a crossover temperature of $T_0 \sim 15$ K was identified where the nature of the spin dynamics changes. At higher temperature, the dynamics consists of thermally activated single spin flips between the two states of the ground state doublet.[24] On cooling below $T < T_0$ the dynamics become independent of temperature, until the time scale sharply rises again below 2 K when the system freezes completely.[25] It was suggested that in the lower temperature regime a quantum relaxation process is involved originating from the slowly fluctuating dipolar magnetic field.

Introducing nonmagnetic impurities often has important effects in geometrically frustrated magnets. In the context of pyrochlore physics, such studies have been presented by Snyder *et al.* for $Dy_{2-x}M_xTi_2O_7$, $M=(Y,Lu)$,[26,27] and by Keren *et al.* for the $Tb_{2-x}Y_xTi_2O_7$ system.[28] For diluted DTO it was found that up to $x \simeq 0.4$ the very narrow distribution of spin relaxation times becomes only slightly broadened, and that the 15 K peak in ac susceptibility does not shift but gradually disappears with doping. In the $Tb_{2-x}Y_xTi_2O_7$ system, dilution slows down the spin dynamics (which persists to $T \to 0$) and gives rise to partial spin freezing.

For our study, samples of $Ho_{2-x}Y_xTi_2O_7$ with $0.1 \leq x \leq 1.8$ were prepared by the usual solid state reaction. X-ray powder diffraction at room temperature confirmed the face centered cubic crystal structure. The neutron spin echo (NSE)[29–31] experiments were performed at the IN11 spectrometer at ILL, Grenoble, and at the NSE spectrometer at NIST, Gaithersburg. Both experiments used a neutron wavelength of $\lambda = 6$ Å. In the ILL experiment a multidetector was

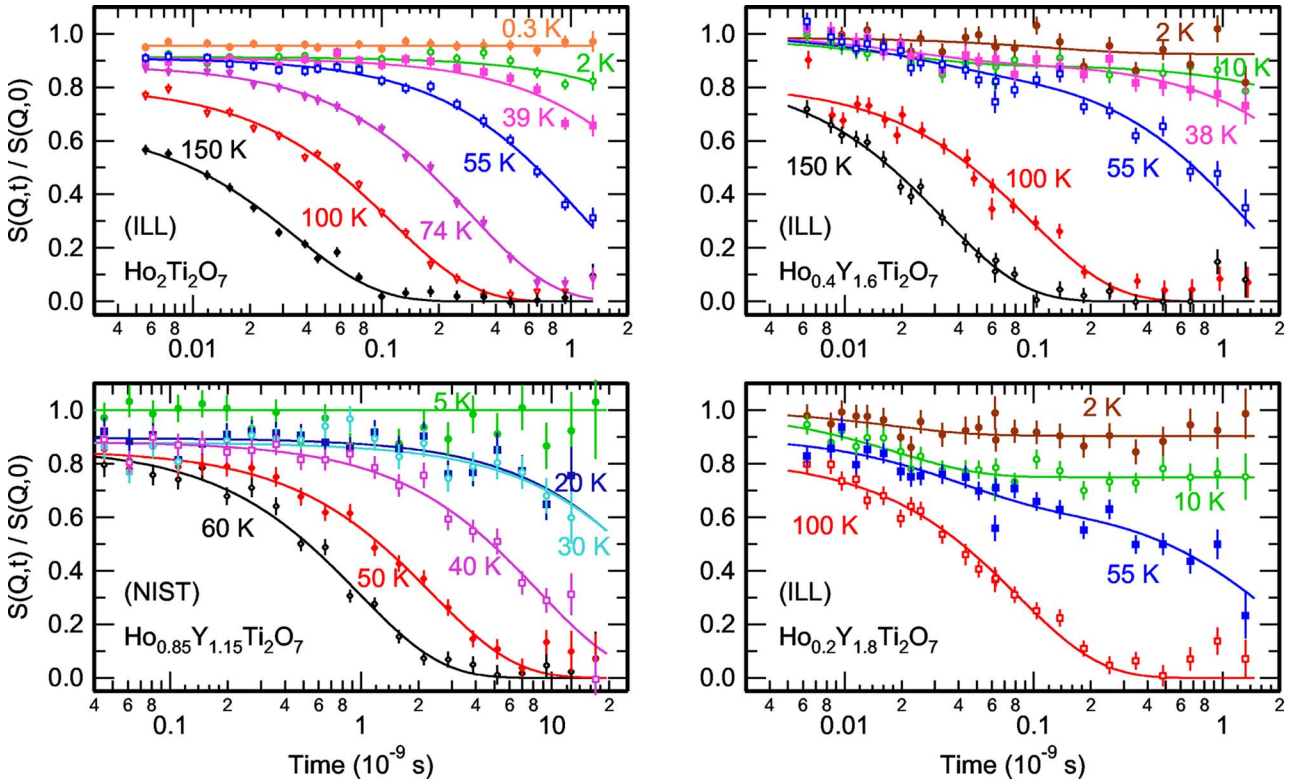

FIG. 2. (Color online) The normalized intermediate scattering function $S(Q,t)/S(Q,0)$ for four samples (including the pure spin ice) at different temperatures. Lines are fits to single or double exponential relaxation functions (see text). Note that the time axis in the bottom left-hand panel is different. The NIST experiment reached a correlation time of 2×10^{-8} s, 10 times longer than at IN11.

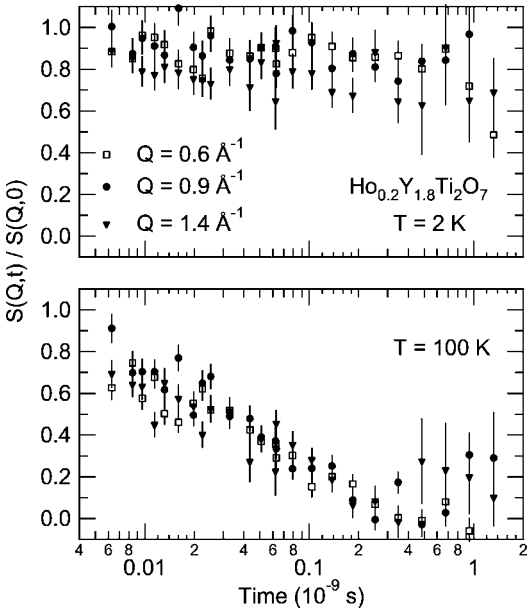

FIG. 3. The normalized intermediate scattering function $S(Q,t)/S(Q,0)$ at two different temperatures for the sample with highest doping ($x=1.8$) showing the absence of Q-dependence in the dynamics.

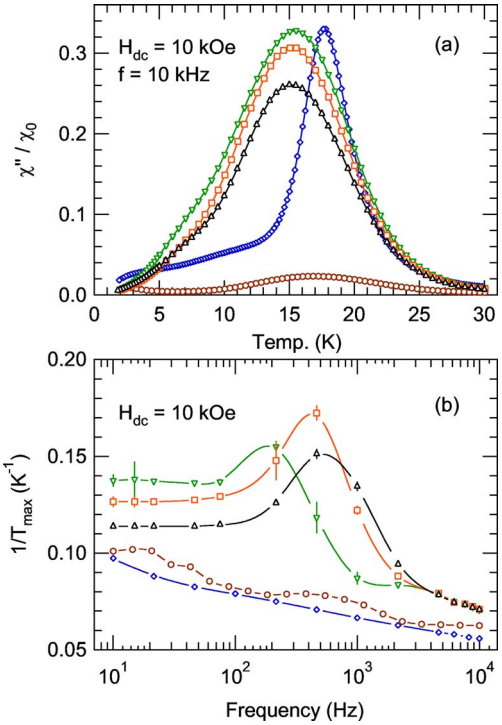

FIG. 4. (Color online) The ac susceptibility of $x=1.8$ (∇), $x=1.5$ (□), and $x=1.3$ (△) samples, together with data of pure HTO (○) and DTO (◇) for comparison. Upper panel (a) imaginary part of ac susceptibility normalized to dc susceptibility. Lower panel (b) inverse of the temperature where the main peak in the imaginary part of ac susceptibility occurs. Lines are guides to the eye.

used, covering a Q range of $0.5\ \text{Å}^{-1} \leq Q \leq 1.6\ \text{Å}^{-1}$. The NIST experiment was set up at $Q=0.4\ \text{Å}^{-1}$ (single detector). Instrumental resolution was measured with the samples at very low temperature (typically in the 100–400 mK range), where it was safe to assume that all dynamical processes on the present time scale are frozen.

Figure 2 shows the measured intermediate scattering function $S(Q,t)/S(Q,0)$ of selected samples. For low doping, $x \leq 1.3$ and lower, the measurements show a Q-independent single exponential spin relaxation in time,

$$\frac{S(Q,t)}{S(Q,0)} = A \exp[-t/\tau(T)],$$

confirming a very narrow distribution of individual relaxation times τ without signs of broadening. For high doping, $x=1.6$ and higher, we find a double exponential relaxation. The *faster* component (again without apparent dependence on Q, see Fig. 3) is new and will be discussed further below. The *slower* component is identical to the single process observed at lower doping. The relaxation times of this process are independent of chemical composition and identical to what was found earlier in pure spin ice. This is further illustrated in the inset of Fig. 5, which shows the same linear relationship between the inverse measurement temperature and the inverse relaxation times $\tau(T)$ of all samples measured by NSE.

A line fit of all available data in the temperature range between 40 K and 200 K to

$$\tau(T) = \tau_0 \exp\left(\frac{\Delta}{k_B T}\right)$$

yields $\tau_0=(7.3\pm1.0)\times10^{-3}$ ns, corresponding to an attempt frequency $\Gamma_0=1/2\tau_0=(6.9\pm1.0)\times10^{10}$ Hz, and an activation energy of $\Delta=(270\pm8)$ K, which is about the value of the CEF splitting.

The two quantities $S(Q,0)$ and $S(Q,t)$ are measured independently in two separate steps in the experiment. $S(Q,0)$ is the scattered magnetic intensity identified through polarization analysis (the spectrometer is run as a diffractometer). $S(Q,t)$ is the dynamic scattering function (spectrometer in "echo" mode) summing up the time-dependent correlations of all spins at time t. The amplitude A of the fit curves of Fig. 2 (as the $t\to0$ limit) thus represents the fraction of the spins participating in the dynamics on the particular time scale of the experiment. The fact that $A\simeq1$ proves that *essentially all* spins participate in the dynamics ($A<1$ would mean that a part of the spin system relaxes in a faster process outside the measurement window). Note that, at increasing temperature, a decrease of the susceptibility is not reflected in A because it affects both $S(Q,t)$ and $S(Q,0)$ to the same extent.[34] Since dilution has no effect on this process (at least up to $x=1.8$), it is straightforward to conclude that between 40 K and 200 K the spin dynamics consists of thermally activated spin flips between the two states of the ground state doublet.

We turn now to a discussion of the *faster* component in the spin dynamics observed at high doping. This process is visible up to relatively high temperature, $T\sim55$ K when nonmagnetic Y occupies over 80% of the magnetic sublattice. With the existing data one can conclude that there is very little temperature dependence of the relaxation time ($\tau=0.01-0.03$ ns) when this process is visible, so that it does

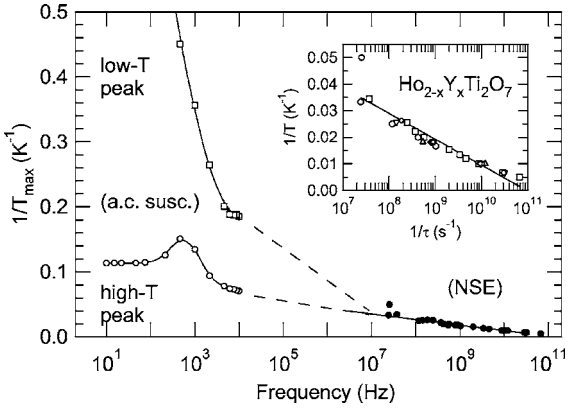

FIG. 5. Combination of neutron spin echo and ac susceptibility results. This graph shows the inverse of the temperatures at which maxima in the imaginary part of the susceptibility occur, as a function of the probing frequency, for the $x=1.3$ sample (the others are qualitatively similar, see Fig. 4). The "high-T" peak of the susceptibility is dominant, and in the 10^3-10^4 Hz range the slope of the curve corresponds to a gap of $\Delta\sim100$ K. For the spin echo frequency range the inverse measurement temperature is plotted against the inverse of the spin relaxation time. The inset shows the NSE data alone for better visibility, for the $x=1.8$ (△), $x=1.6$ (◇), $x=1.15$ (○), $x=1.1$ (▽), $x=0.7$ (◁), and $x=0$ (□), samples, revealing Arrhenius nature in the temperature range between 40 K and 200 K. The slope of the curve of the NSE data corresponds to $\Delta\sim270$ K.

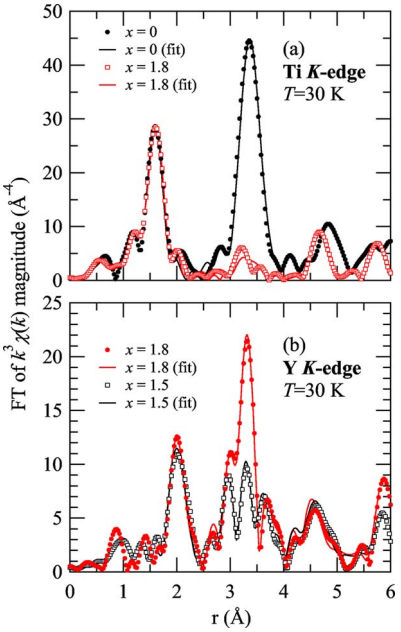

FIG. 6. (Color online) Fourier transform (FT) magnitudes of the $k^3\chi(k)$ EXAFS data for some $Ho_{2-x}Y_xTi_2O_7$ samples at the (a) Ti K edge and (b) the Y K edge. These data were collected at 30 K. Data are transformed from 2.5 to 16.0 $Å^{-1}$ and Gaussian narrowed by 0.3 $Å^{-1}$. The fit ranges are from 1.4 to 4.0 Å in the upper panel and from 1.6 to 5.9 Å in the lower panel, respectively.

not appear to be thermally activated. It is also clear that a relatively small spectral weight w ($w\sim0.05-0.1$ for $x=1.6$, $w\sim0.1-0.2$ for $x=1.8$) is involved in the signal.

The low spectral weight can be interpreted in two different ways. First, the fast process may correspond to a movement which is confined to a narrow cone around a local [111] axis, so that the individual spin loses only little self-correlation in the relaxation process (but all spins may participate). Second, the process may just as well consist of real spin flips, in which case only a small number of spins participate (to account for the low spectral weight). These spins would have to exist in a unique environment, for instance on the B site of the pyrochlore structure which is occupied by Ti. The fact that the spectral weight w increases with increasing temperature (see lower right-hand panel in Fig. 2) makes the first assumption more likely, but does not preclude the second.

To complement the NSE studies, ac susceptibility measurements have been performed on a couple of $Ho_{2-x}Y_xTi_2O_7$ powder samples and on single-crystal samples of HTO and DTO, in an external field up to 1 T, using commercially available fully calibrated magnetic measurement equipment. Bulk susceptibility measurements probe at much lower frequencies than neutron scattering, giving access to the dynamics of these systems at correspondingly lower temperatures.

As Fig. 4 shows, the diluted samples beyond the percolation limit ($Ho_{0.78}Y_{1.22}Ti_2O_7$) reveal the $T_0\sim15$ K peak much clearer than pure HTO. This peak was shown to correspond to the main relaxation process seen in NSE.[24] In pure HTO the peak is smaller compared to the other concentrations because the attempt frequencies of the thermally activated Arrhenius and the slower quantum processes are relatively close in this temperature range. In DTO the same peak comes out more clearly because the quantum process is intrinsically slower and sets in at a lower temperature. Generally, the imaginary part of the susceptibility also shows a second peak at lower temperature which is significantly less pronounced than the main peak.

An important result of the present work is that the Arrhenius behavior discussed above is modified below $T\sim20$ K in the ac susceptibility (see Fig. 5). For frequencies in the 10^3-10^4 Hz range in the ac susceptibility, the shift of the main peak is still consistent with Arrhenius behavior and a gap of $\Delta\sim100$ K. This value is substantially different than the neutron value quoted above (270 K). This does not necessarily imply a change in the crystal field level scheme, rather it suggests the coexistence of two processes with similar time scales but different thermal evolution. At lower frequency the position of the main peak in ac susceptibility then becomes independent of temperature and the low temperature peak moves out of the measurement window of our apparatus. This indicates the existence of a quantum relaxation process which becomes dominant at low temperature where the thermal main process freezes and becomes inactive.

A measurement of ac susceptibility on diluted DTO samples[26] revealed similar complexity in this system. The authors found a gap $\Delta\sim210$ K for low doping up to $x\sim1.0$ and an increase of the gap to about $\Delta\sim310$ K when the doping was further increased to $x=1.98$.

To confirm the local atomic structure of our samples, extended x-ray absorption fine structure (EXAFS) spectra were

collected at the Ho L_{III}, Y K, and Ti K edges on BL 10-2 and BL 11-2 at the Stanford Synchrotron Radiation Laboratory (SSRL) in transmission mode on samples with $x=0$, 1.3, 1.4, 1.5, and 1.8 between 30 and 300 K. All samples were prepared and data reduced and fit using methods similar to those described in Refs. 32 and 33.

The first peak in the Ti K-edge (FT) of the k^3-weighted EXAFS function $\chi(k)$ [Fig. 6(a)] corresponds to the 6 Ti-O neighbors at 1.956(7) Å. Note that peak positions in such transforms include a calculable phase shift of the photoelectron at the absorbing and backscattering sites, causing, in this case, the peak to appear at ~1.6 Å in the transform. The amplitude is proportional to the number of Ti-O(1) pairs, as well as depending on the distribution width of the bond lengths. These measurements indicate that the Ti-O(1) environment is nearly identical in $Ho_2Ti_2O_7$ and the $x=1.8$ sample, and we conclude that no more than 2% of the Ti atoms are in a different oxygen environment. The same is true of the Y edge data shown in Fig. 6(b), except that the first peak is a combination of two Y-O(2) pairs at 2.186(6) Å and six Y-O(1) pairs at 2.476(5) Å, as expected from the nominal crystal structure. These somewhat longer pair distances cause the oxygen peaks to overlap slightly more with the Y-Ti/Ho/Y pairs at 3.57 Å, creating the slight observed reduction in the first oxygen peak. Therefore, the fits indicate the oxygen environment around Y in these samples is identical within the estimated errors.

The biggest changes in the EXAFS signal are in the range between about 2.5 and 4 Å in the transform. The main contribution to this signal is similar for all three edges (Ho L_{III}-edge data is not shown), namely each absorbing metallic atom nominally has six Ti, $3(2-x)$ Ho and $3x$ Y neighbors at the same distance (3.57 Å). Because each of these atomic species has strong differences in the backscattering phase, strong interferences occur that create a very complicated pattern in the FT. However, as shown in Fig. 6(b), these data are nevertheless fit very well by the nominal model. The Y K-edge data are particularly sensitive to the relative fraction of Ho and Y species in this scattering shell, and we obtain a result that agrees with the nominal concentration within 5%. These data therefore indicate that the Y and Ho atoms are very well mixed within these materials, with little if any clustering of the substituting species. Taken together with the Ti edge result mentioned above, these data rule out any significant ($\gtrsim 5\%$) subset of Ho atoms on Ti sites. The results from the Ho edge data, while less constraining, agree with this deduction. We therefore rule out any phase impurity of this kind on the scale of the 10–20% spectral weight necessary to explain the fast component of the $x=1.8$ NSE data with a lattice mechanism.

To conclude, we have found remarkably little effect of doping (up to 90%) with nonmagnetic Y on the dynamics of $Ho_2Ti_2O_7$. The Ho^{3+} ion experiences little change in the crystal field, and its spin dynamics is unaltered. The distribution of individual spin relaxation times is very narrow and independent of the doping. All spins participate in the dynamics. At the highest Y doping, another fast relaxation mechanism appears with a small weight in the neutron scattering data. EXAFS shows that this process is not due to dislocated Ho^{3+} ions on the Ti site, hence it is intrinsic to the Ho site. It cannot fully relax the spin, so it appears to be a wobblelike relaxation process of the spin in a narrow cone. Susceptibility measurements show that at low temperatures, where the dynamics is too slow for the NSE technique, the Arrhenius behavior is masked by another dynamical process with very little temperature dependence.

The authors thank S. Pujol (ILL) and R. W. Erwin (NIST) for their help in setting up the low temperature equipment in the neutron scattering experiments. This work is supported by the Spallation Neutron Source Project (SNS). SNS is managed by UT-Battelle, LLC, under Contract No. DE-AC05-00OR22725 for the U.S. Department of Energy (DOE). Work at Brookhaven was supported by the Division of Material Sciences, U.S. DOE under Contract No. DE-AC02-98CH10886. This work utilized facilities supported in part by the National Science Foundation under Contract No. DMR-0454672. Work at Lawrence Berkeley National Laboratory was supported by the Director, Office of Science, Office of Basic Energy Sciences (OBES), of the U.S. DOE under Contract No. DE-AC02-05CH11231. Two of the authors (J.S.G. and S.T.B.) were partially supported by a NATO Collaborative Linkage Grant, reference number PST.CLG.978705. Portions of this research were carried out at SSRL, a national user facility operated by Stanford University on behalf of the U.S. DOE, OBES. Work at UNLV was supported by the U.S. Department of Energy Cooperative Grant No. DE-FC52-01NV14049.

[1] A. P. Ramirez, Annu. Rev. Mater. Sci. **24**, 453 (1994); in *Handbook of Magnetic Materials*, edited by K. H. J. Buschow (Elsevier, Amsterdam, 2001), Vol. 13, Chap. 4.

[2] *Frustrated Spin Systems*, edited by H. T. Diep (World Scientific, Singapore, 2004).

[3] J. S. Gardner, S. R. Dunsiger, B. D. Gaulin, M. J. P. Gingras, J. E. Greedan, R. F. Kiefl, M. D. Lumsden, W. A. MacFarlane, N. P. Raju, J. E. Sonier, I. Swainson and Z. Tun, Phys. Rev. Lett. **82**, 1012 (1999).

[4] J. D. M. Champion, A. S. Wills, T. Fennell, S. T. Bramwell, J. S. Gardner, and M. A. Green, Phys. Rev. B **64**, 140407(R) (2001).

[5] J. R. Stewart, G. Ehlers, A. S. Wills, S. T. Bramwell, and J. S. Gardner, J. Phys.: Condens. Matter **16**, L321 (2004).

[6] H. Sakai, K. Yoshimura, H. Ohno, H. Kato, S. Kambe, R. E. Walstedt, T. D. Matsuda, Y. Haga, and Y. Onuki, J. Phys.: Condens. Matter **13**, L785 (2001).

[7] M. J. Harris, S. T. Bramwell, D. F. McMorrow, T. Zeiske, and K. W. Godfrey, Phys. Rev. Lett. **79**, 2554 (1997).

[8] A. P. Ramirez, A. Hayashi, R. J. Cava, R. Siddharthan, and B. S. Shastry, Nature (London) **399**, 333 (1999).

[9] J. Snyder, J. S. Slusky, R. J. Cava, and P. Schiffer, Nature (London) **413**, 48 (2001).
[10] S. T. Bramwell and M. J. P. Gingras, Science **294**, 1495 (2001).
[11] B. C. den Hertog and M. J. P. Gingras, Phys. Rev. Lett. **84**, 3430 (2000).
[12] S. T. Bramwell, M. J. Harris, B. C. den Hertog, M. J. P. Gingras, J. S. Gardner, D. F. McMorrow, A. R. Wildes, A. Cornelius, J. D. M. Champion, R. G. Melko, and T. Fennell, Phys. Rev. Lett. **87**, 047205 (2001).
[13] R. G. Melko, B. C. den Hertog, and M. J. P. Gingras, Phys. Rev. Lett. **87**, 067203 (2001).
[14] T. Sakakibara, T. Tayama, Z. Hiroi, K. Matsuhira, and S. Takagi, Phys. Rev. Lett. **90**, 207205 (2003).
[15] J. Snyder, B. G. Ueland, J. S. Slusky, H. Karunadasa, R. J. Cava, Ari Mizel, and P. Schiffer, Phys. Rev. Lett. **91**, 107201 (2003).
[16] L. G. Mamsurova, K. K. Pukhov, N. G. Trusevich, and L. G. Shcherbakova, Sov. Phys. Solid State **27**, 1214 (1985).
[17] Y. M. Jana and D. Ghosh, Phys. Rev. B **61**, 9657 (2000).
[18] S. Rosenkranz, A. P. Ramirez, A. Hayashi, R. J. Cava, R. Siddharthan, and B. S. Shastry, J. Appl. Phys. **87**, 5914 (2000).
[19] W. F. Giauque and J. W. Stout, J. Am. Chem. Soc. **58**, 1144 (1936).
[20] L. Pauling, *The Nature of the Chemical Bond* (Cornell University Press, Ithaca, NY, 1945).
[21] V. F. Petrenko and R. W. Whitworth, *Physics of Ice* (Clarendon, Oxford, 1999).
[22] K. Matsuhira, Y. Hinatsu, K. Tenya, and T. Sakakibara, J. Phys.: Condens. Matter **12**, L649 (2000).
[23] K. Matsuhira, Y. Hinatsu, and T. Sakakibara, J. Phys.: Condens. Matter **13**, L737 (2001).
[24] G. Ehlers, A. L. Cornelius, M. Orendáč, M. Krajňaková, T. Fennell, S. T. Bramwell, and J. S. Gardner, J. Phys.: Condens. Matter **15**, L9 (2003).
[25] J. Snyder, B. G. Ueland, J. S. Slusky, H. Karunadasa, R. J. Cava, and P. Schiffer, Phys. Rev. B **69**, 064414 (2004).
[26] J. Snyder, S. Slusky, R. J. Cava, and P. Schiffer, Phys. Rev. B **66**, 064432 (2002).
[27] J. Snyder, B. G. Ueland, A. Mizel, J. S. Slusky, H. Karunadasa, R. J. Cava, and P. Schiffer, Phys. Rev. B **70**, 184431 (2004).
[28] A. Keren, J. S. Gardner, G. Ehlers, A. Fukaya, E. Segal, and Y. J. Uemura, Phys. Rev. Lett. **92**, 107204 (2004).
[29] *Neutron Spin Echo*, in Lecture Notes in Physics Vol. 128, edited by F. Mezei (Springer, Berlin, 1979).
[30] *Neutron Spin Echo*, in Lecture Notes in Physics Vol. 601, edited by F. Mezei, C. Pappas, and T. Gutberlet (Springer, Berlin, 2002).
[31] H. Casalta, P. Schleger, C. Bellouard, M. Hennion, I. Mirebeau, G. Ehlers, B. Farago, J. L. Dormann, M. Kelsch, M. Linde, and F. Phillipp, Phys. Rev. Lett. **82**, 1301 (1999).
[32] C. H. Booth, J. S. Gardner, G. H. Kwei, R. H. Heffner, F. Bridges, and M. A. Subramanian, Phys. Rev. B **62**, R755 (2000).
[33] S.-W. Han, J. S. Gardner, and C. H. Booth, Phys. Rev. B **69**, 024416 (2004).
[34] This holds at temperatures below $T \simeq 200$ K. A closer inspection of the data shows a strong decrease of A at $T > 200$ K, which is due to the increased population of higher CEF states. This gives rise to inelastic scattering which is not accounted for in the intermediate scattering function which describes only quasielastic scattering.